Fire Safety Journal 44 (2009) 363–369

Contents lists available at ScienceDirect

Fire Safety Journal

journal homepage: www.elsevier.com/locate/firesaf

Implications of droplet breakup and formation of ultra fine mist in blast mitigation

K.C. Adiga [a,*], Heather D. Willauer [b], Ramagopal Ananth [b], Frederick W. Williams [b]

[a] NanoMist Systems, LLC, 2260 7th Street, Macon, GA 31206, USA
[b] The Navy Technology Center for Safety and Survivability, Chemistry Division, Naval Research Laboratory, Washington, DC 20375-5320, USA

ARTICLE INFO

Article history:
Received 7 June 2007
Received in revised form
18 August 2008
Accepted 19 August 2008
Available online 2 October 2008

Keywords:
Blast mitigation
Droplet breakup
Energy extraction
Ultra fine mist
Vaporization energy
Shock weakening

ABSTRACT

Blast-induced droplet breakup producing ultra fine water mist process was examined in view of assessing its implications on blast mitigation. An earlier review proposed that droplet breakup process, amongst other implications, may weaken the shock due to breakup energy absorption. In this work, droplet breakup energies for water droplets have been determined from the surface energies of both parent and child droplets. A breakup energy of 18 J/kg was required to fragment a 0.5 mm parent droplet into 10,000 mono-dispersed child droplets. Compared to the vaporization energy of 2.25 MJ/kg, the droplet breakup energy was found not significant in weakening the shock. While the droplet deformation energy and curvature effects could increase the breakup energy, its overall contribution to the total energy extraction was not as significant as the latent heat of vaporization. Further, the analysis shows about 22-fold increase in surface area of the child droplets. The study revealed the surface-to-volume ratio of the ultra fine droplets and their vaporization timescale should be well positioned for shock energy extraction.

1. Introduction

The US Navy has recognized the benefits of water mist for fire suppression [1,2], and as a result these systems have been installed in the Navy's latest class of amphibious ships, the *San Antonio* class (LPD-17). As these systems are being included in more ship designs, there is a desire to investigate their potential use in limiting the primary damage area (PDA) caused by an explosion from a weapon or terrorist attack [3–5]. Many reports have cited mitigation of condensed-phase explosions and vapor cloud explosions using water mist, and a few have addressed some of the plausible mechanisms by which mitigation was achieved [3,5]. These include the extraction of energy from both the shock front and the chemical reaction zone when water droplets fragment and evaporate [3,5]. The water mist droplet size and concentration, the chemical composition of the explosive (missile, TNT, dust cloud), and the geometric complexity of the area being mitigated determine how well the water droplet interaction promotes energy absorption and thus mitigation.

Ideally, a shipboard water mist system would mitigate the initial blast overpressures and any quasi-static overpressures and secondary effects caused by a blast. Shipboard environments are geometrically complex, consisting of multiple compartments ranging in size and containing varying degrees of congestion. A few reports suggest that a blast in this type of environment could actually enhance the overpressures due to the reflection of shock waves [3]. The other issues are the time, the amount of water, and water droplet size needed to achieve mitigation in the event of an incident.

The Naval Research Laboratory (NRL) was sponsored by the Office of Naval Research (ONR) to study these issues by conducting a series of small-scale blast mitigation tests in the summer of 2005 [6]. The tests were carried out in a bombproof shelter at the Naval Surface Warfare Center (NSWC), Indian Head, Maryland using TNT. In the TNT blast experiments, the quasi-static pressure produced by the detonation of a 5 lb (2.2 kg TNT) charge of TNT was reduced by as much as 47%. Approximately 27 liters of water was injected into a compartment whose inside dimensions were 4.6 m × 4.6 m × 3.1 m (15.1 ft × 15.1 ft × 10.1 ft). The water mist characterization studies indicated that mitigation was achieved with droplet sizes ranging from 35 to 550 μm with a Sauter mean diameter (SMD) >50 μm and a mass loading of 76–87 g/m^3 [7]. Thus, only about 18–21% of the 412 g/m^3 was suspended at any given time in the test series. This is likely the result of droplets settling to the floor and along the chamber walls. SMD is the diameter of the droplet whose surface to volume ratio is equal to that of the entire spray [8].

The results of the blast mitigation studies suggest that there are other mechanisms, in addition to water droplet fragmentation and evaporation [3,5], by which water mist mitigates the blasts.

* Corresponding author. Tel.: +1 478 750 4411.
E-mail address: kcadiga@nanomist.com (K.C. Adiga).

0379-7112/$ - see front matter © 2008 Elsevier Ltd. All rights reserved.
doi:10.1016/j.firesaf.2008.08.003

Nomenclature

d	diameter
d_c	maximum diameter
$d_{initial}$	initial diameter of the droplet (m)
D	diffusion coefficient (m^2/s)
E_p or e_p	surface energy of parent droplet (J)
E_c or e_c	surface energy of child droplets (J)
$m_{vap,o}$	mass fraction of water vapor in the mixture.
$m_{vap,\infty}$	mass fraction of water vapor away from surface
Oh	Ohnesorge number $= \mu/(\rho d\sigma)^{0.5}$
S_p	surface area of a parent droplet (m^2)
S_c	surface area of child droplet (m^2)
t_{vap}	evaporation time (s)
U	velocity (m/s)
V	relative velocity (m/s)
We	Weber number $= \rho V/d\sigma$
σ	surface tension, water 7.2×10^{-2} N/m
ρ	density of fluid (kg/m^3)
ρ_l	liquid water density $= 1000\,kg/m^3$
Γ	exchange coefficient $= D\rho$ (kg/m s)
Γ_{vap}	water vapor exchange coefficient (kg/m s) $= 2.6 \times 10^5$ kg/m s

We propose a comprehensive set of mechanism of interactions. Fig. 1 shows a schematic of the proposed interaction of water droplets in the detonation process. The water mist (parent droplets) is essentially unaffected by the incoming shock wave. Once the front has passed, the droplets enter an environment where the air is moving at supersonic velocities. These forces shear the coarse parent droplets into smaller droplets (child droplets) and energy is absorbed from the shock front. The child droplets produced can interact with the shock front, the reaction front, and the reaction product zone (Fig. 1) by other mechanisms in addition to evaporation to absorb energy from the blast.

Behind the shock front, the small droplets are rapidly accelerated to the shock velocity and absorb kinetic energy from the blast, as there is a transfer of momentum from the gas phase to the water phase. When the droplets penetrate the reaction front, they can absorb radiation and evaporate, causing further weakening of the blast. If the droplets reach the reaction products zone, more evaporation may occur, resulting in slowing down the expansion and absorption processes.

The chemical composition of high explosives and its amount determine the time scales for the shock and reaction front propagation. Water mist droplet size plays a key role in determining the time scales for droplet breakup, momentum transfer, evaporation, and radiation absorption. Blast-induced droplet breakup process is critical to producing child droplets capable of penetrating the different blast zones to achieve mitigation by latent heat and kinetic energy absorption. A number of recent studies are available that evaluate the effect of ultra fine mist (UFM) on cooling and suppression of fires [15–19].

An earlier review [3] proposed that droplet breakup process, amongst other implications, may weaken the shock due to the breakup energy absorption. The objective of this work was to assess the implication of droplet breakup process, first by estimating the magnitudes of breakup energy. The breakup energies for various schemes of droplet size and number of droplets are compared with the droplet vaporization energies and their timescales using analytical tools. The overall emphasis is to identify and understand the factors affecting the blast mitigation process using water mist. This knowledge can be used to optimize and engineer future Navy ship-wide water mist systems having the capability of acting as both a fire suppression system and a blast mitigation system.

2. Background

The aerodynamic droplet breakup process in water spray blast mitigation is an attractive beneficial feature for technology development. This blast-induced droplet breakup occurs due to local acceleration of the gas and the coarse water droplet acceleration. The droplet breakup dominates when the relative velocity between the gas and droplet develops, so that the droplet Weber number is more than 12 for a sufficient time [3,9–14]. The process has been demonstrated in reduced scale experiments as well as in limited large-scale tests.

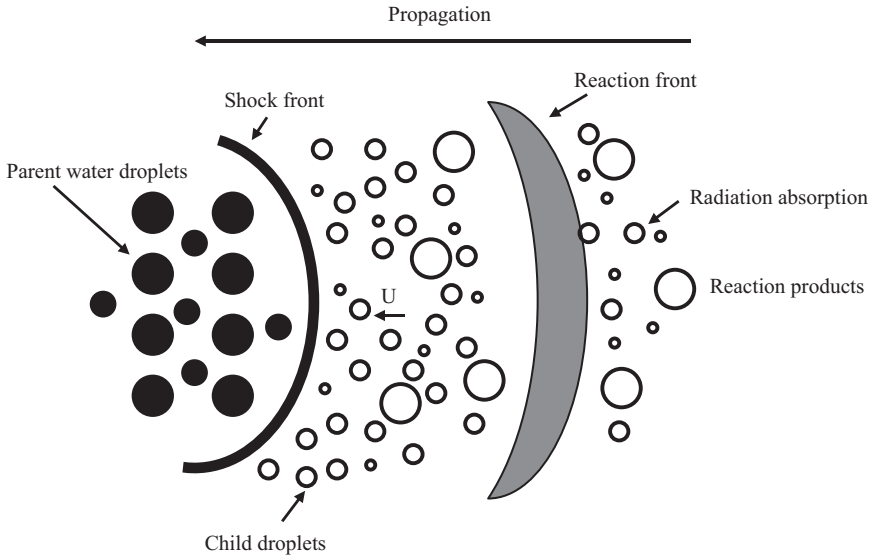

Fig. 1. Interaction of water droplets in detonation process.

The Weber number, *We*, is

$$We = \rho V^2 d/\sigma \quad (1)$$

In this equation, ρ is the density of the fluid, V is the initial relative velocity between the flow field and the droplet, d is the initial diameter of the droplet and σ is the surface tension of the liquid. The mechanism of droplet fragmentation depends on the Weber number of the parent droplet. The mechanistic pathways to final child droplets generally observed for droplets in the gas flow field are listed below:

- Vibration breakup $We < 12$
- Bag breakup $12 < We < 50$
- Bag-and-stamen breakup $50 < We < 100$
- Sheet stripping $100 < We < 350$
- Wave crest stripping followed by catastrophic breakup $We > 350$

A schematic of this mechanism is shown and described by Pilch and Erdman [14].

As an example, coarse precursor droplets of 1–5 mm (1000–5000 μm) are fragmented into 20–30 μm. The fragmentation efficiency is dependent upon the droplet flow rate, initial droplet size and concentrations. The UFM (child droplets) formed by the breakup process is a powerful blast mitigation agent. The vaporization energy by the ultra fine water mist is one of the sources of energy extraction from the shock. This analysis evaluates the time scales and relative contributions these two processes have on weakening the shock.

3. Results

3.1. Analysis of breakup process and computing energies

First, a simple droplet breakup process, without referring to mechanisms, is shown schematically in Fig. 2 in terms of initial and final states. In this simple schematic, the droplet first deforms and elongates under flow-induced stress. This initial state (State 1) and the final state (State 2) are related to the droplet's properties such as diameter, surface area, and surface energies, as shown in Fig. 2.

As a first approximation, the energy associated with the breaking of a single droplet into several child droplets will be computed based on the surface energy difference between State 1 and State 2. There is a formation route or path in between these two states. For example, before the droplet breaks up, the drops deform and reach an ellipsoidal shape similar to that of an oblate spheroid. Such a mechanistic pathway imposes an activation route with an energy barrier to pass through before coming to State 2. The implication of this will be reviewed and an order of magnitude analysis will be provided later.

Under favorable conditions, the initial droplet will break into a larger number of child droplets behind the shock wave. During the breakup process, there will be a considerable increase in surface area per unit mass of child droplets that in turn will have increased droplet surface energy. The droplet surface energy is computed using the droplet surface area and surface tension of water as follows:

Surface area of a parent droplet S_p of mass m and diameter d is

$$S_p = \pi d^2 \quad (2)$$

State 1: Surface energy E_p of a parent droplet of diameter d is

$$E_p = \pi d^2 \sigma \quad (3)$$

where σ is the surface tension of water.

The total surface area S of child droplets of total mass m and diameters d_1, d_2, d_3, …, d_n is

$$S = \pi(d_1^2 + d_2^2 + \cdots + d_n^2) \quad (4)$$

State 2: Total surface energy of child droplets, E_c, of total mass m (kg) is

$$E_c = \pi\sigma(d_1^2 + d_2^2 + \cdots + d_n^2) = S\sigma \quad (5)$$

The surface energy difference between the final state (State 2) and the initial state (State 1) per unit mass Eqs. (3) and (5) is

$$\Delta E = (E_c - E_p)/\mathrm{m}\ (\mathrm{J/kg}) \quad (6)$$

This is the energy required to break the parent droplet into "n" number of child droplets per unit mass of droplet.

Results are shown in Fig. 3 for a parent (initial) droplet with a 500 μm diameter (0.5 mm) (corresponding to 6.54×10^{-8} kg) breaking up into ~10,000 child droplets. Here, the cascading breakup effects are not considered, namely the parent droplet directly goes to a child droplet as opposed to intermediate stages, which are not shown.

Fig. 3 shows how the diameter of the child droplets decreases as a function of the number of fragments formed. For about 10,000 fragments, the final droplet size is close to 23 μm. These are mono-disperse droplets. Calculations can be done using Monte

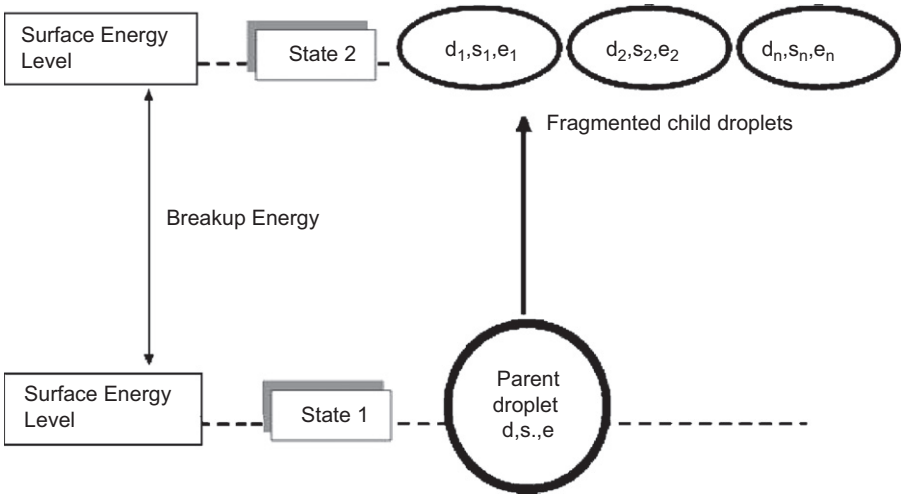

Fig. 2. Various surface energy states for droplet breakup into child droplets.

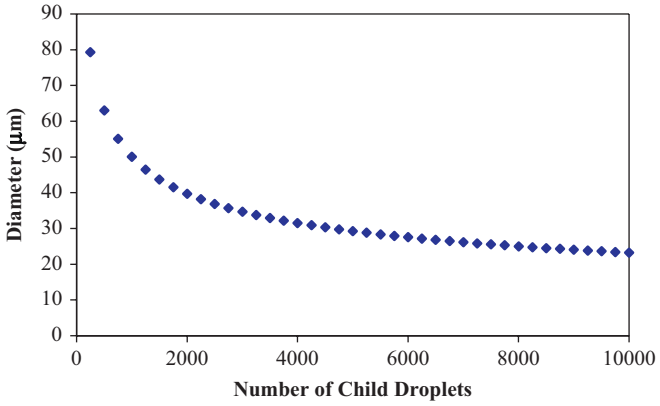

Fig. 3. Diameter of child droplets as a function of number of fragments formed. Initial droplet diameter, 500 μm.

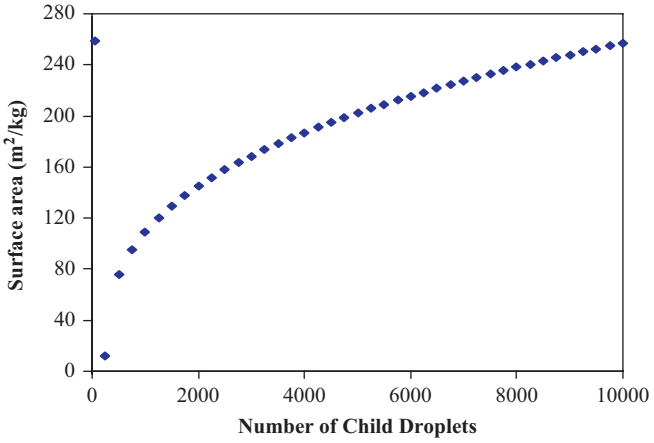

Fig. 4. Variation of surface area as a function of number of droplets. Initial diameter, 500 μm, and initial surface area, 12 m^2/kg.

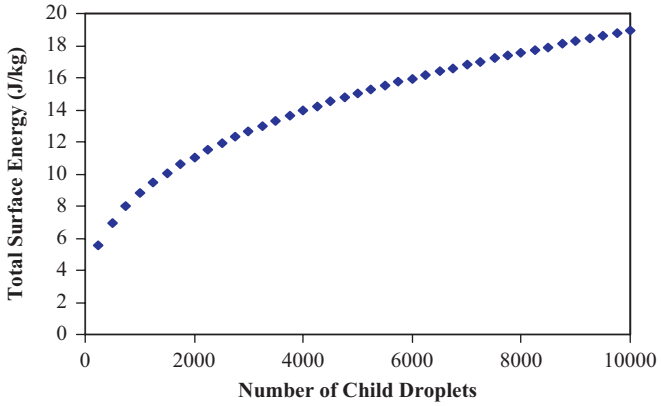

Fig. 5. Surface energy variation with number of child droplets.

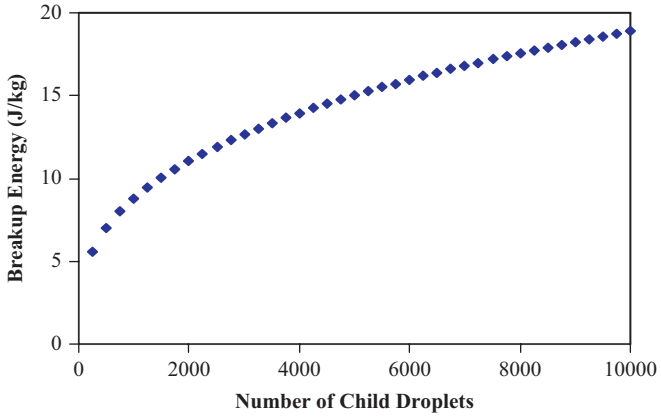

Fig. 6. Breakup energy variation with number of child droplets. Initial droplet diameter, 500 μm.

Carlo methods for a wide range of droplet size distributions. However, this approach is not considered here since, for the calculation of surface energy, all that matters is the total surface area of the final droplets. The droplet fragments formed are just in the right size range for blast mitigation to occur by rapid energy extraction by UFM.

Fig. 4 shows how the surface area per unit mass increases as a function of the number of child droplets. The initial surface area of the parent droplet is 12 m^2/kg, and upon its fragmentation into child droplets the surface area increases to 260 m^2/kg. This ~22-fold increase in surface area of 23 μm mono-dispersed UFM will increase the surface energy of droplets as well as their vaporization rates. The increase in surface area will have two immediate implications: (1) an increase in the surface energy of the child droplets that will be absorbed by the shock, causing more energy extraction and possible weakening of the shock, and (2) rapid vaporization of UFM absorbing 2.25×10^6 J/kg of water.

Fig. 5 shows the surface energies of fragmented droplets, and how it is increased from 0.88 to 18.5 J/kg for 10,000 droplets. This increase in surface energy results from the new surfaces created by the child droplets. This energy has to come from the shock wave. The difference in energies of the parent and the child droplets is shown in Fig. 6. This is the net energy to be extracted from the shock to break the parent droplets. This energy extraction, if significant, could weaken its strength. The total energy extraction is approximately 18 J/kg when the coarse water spray droplets are fragmented into UFM. This magnitude is small compared to 2.25×10^6 J energy extraction by 1 kg of water upon complete vaporization. Thus, the energy budget clearly indicates that the contribution from the breakup process, as compared to latent heat absorption, is not significant. The fragmentation of the parent droplet is, however, very important to the global process. The increase in surface area created by the child droplets will enhance shock energy extraction by reducing the vaporization time scales.

3.2. *Deformation transition energy consideration in breakup process path*

Based on the energy extraction possibilities presented, the magnitude of the droplet breakup energy is far less effective compared to the enthalpy of vaporization of water. The breakup energy is based on the computed surface energy difference between State 1 (parent droplet) and State 2 (child droplets). However, the droplets must go through an energy barrier process before reaching their final state. For example, when a completely spherical droplet is subjected to the flow field, its windward side will have higher pressure compared to the forward stagnation point. Fig. 7 shows a schematic of energy states for parent droplet, child droplets, and the intermediate activation process of deformation.

The droplets first deform into ellipsoid shapes as shown in Fig. 8 before they go through several of the mechanisms illustrated and described by Pilch and Erdman [14]. In the

vibrational type shown for a low Weber number ($We<12$), droplets start necking in and break into two droplets after becoming ellipsoid. This curvature effect will push the surface energy to a higher state before fragmentation occurs, leading to additional energy absorption. This process is not considered important because the Weber number encountered in the detonation field must be higher.

Referring to the bag breakup process described by Pilch and Erdman [14] and illustrated in Fig. 8, there is a significant curvature effect, as the surface goes through ellipsoid and bag. The deformation will add additional surface area. Before the droplet breaks up, the drop deforms and reaches an ellipsoidal shape, similar to that of an oblate spheroid as shown in Fig. 7.

Chryssakis and Assaniss [12] have published descriptions of high Weber number droplet breakup with various deformation profiles for droplets undergoing fragmentation. Hslang and Faeth [13] conducted experiments in a wide range of conditions and showed that the maximum droplet distortion can be expressed as

$$d_c/d = 1 + 0.19We^{1/2}, \quad Oh<0.1,\ We<100 \tag{7}$$

where d is the droplet diameter, d_c is the maximum distorted diameter, and Oh is the Ohnesorge number incorporating the viscosity effects. However, when $We>100$, typical of detonation conditions,

$$d_c/d\sim 2, \quad Oh<0.1,\ We>100 \tag{8}$$

As shown in Fig. 7, the diameter increases to twice the original, but the other diameter also varies. This indicates that the surface area variation and the curvature effects before they fragment will not be significant considering the initial (State 1) and final state (State 2) of a huge number of child droplets. This still is an insignificant amount of energy addition compared to the vaporization energy, which is 2.25×10^6 J/kg of water.

3.3. Energy extraction by vaporization of fragmented droplets and the time scales

The next aspect to be evaluated is the vaporization time scales of these fragmented droplets. For a qualitative judgment of the relative estimate of the droplet size effect on the vaporization behavior, the d^2-law droplet evaporation calculation is used here. This expression does not consider the effects of the coupled flow

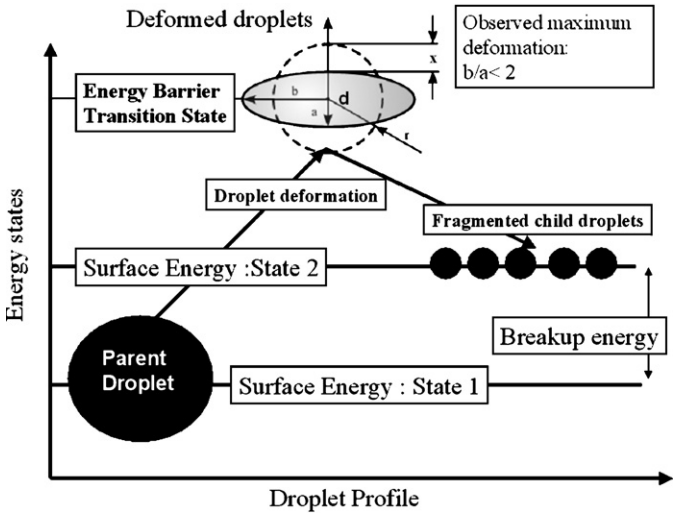

Fig. 7. A schematic of activation process of droplet deformation before reaching the final child droplet stage.

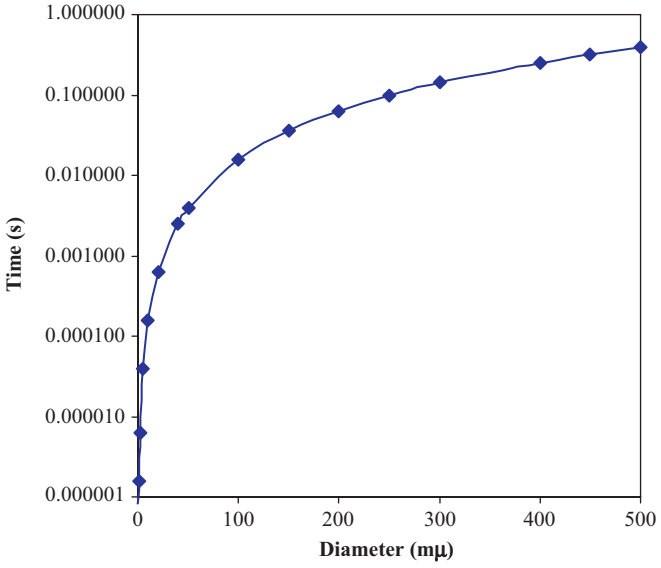

Fig. 9. d^2-law evaporation time scales of child droplets from the shock-induced droplet breakup process. Vaporization time is calculated at 100 °C at 0% humidity.

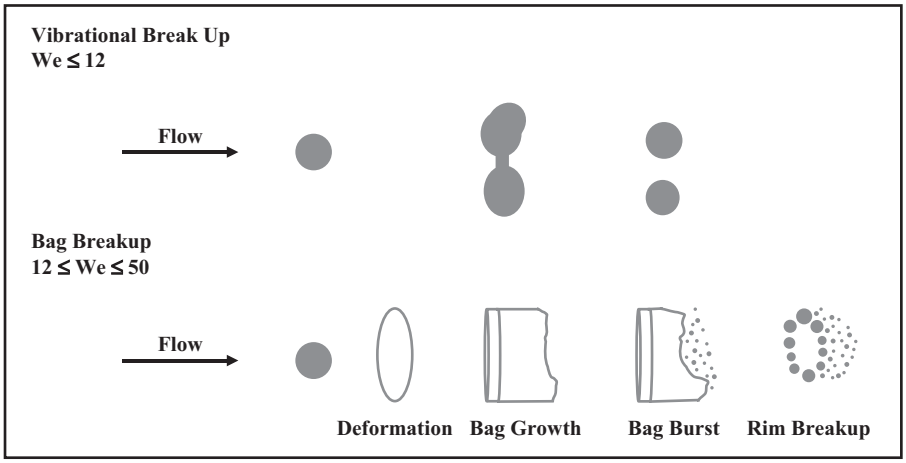

Fig. 8. Droplet breakup mechanisms.

field, heat transfer, and residence time. As such, the approach gives only a qualitative behavior of a single droplet.

The evaporation time of a single droplet of water:

$$t_{vap} = \frac{d_{initial}^2 \rho_l}{8 \Gamma_{vap} \ln\left(1 + \frac{m_{vap,o} - m_{vap,\infty}}{1 - m_{vap,o}}\right)} \quad (9)$$

where

t_{vap} evaporation time (s)
$d_{initial}$ initial diameter of the droplet (m)
ρ_l liquid water density = 1000 kg/m^3
Γ_{vap} water vapor exchange coefficient (kg/m s) = 2.6×10^{-5} kg/m s
Γ exchange coefficient = $D\rho$ (D = vapor diffusion coefficient (m^2/s), ρ is the vapor density (kg/m^3))
$m_{vap,o}$ mass fraction of water vapor in the mixture at temperature T (K) at the droplet surface.
$m_{vap,\infty}$ mass fraction of water vapor away from surface at temperature T (K). In this example, the relative humidity, RH = 0 (dry air). $m_{vap,\infty} = 0$.

The variation of droplet vaporization time as a function of droplet fragments from 0.1 to 500 μm is shown in Fig. 9. Note that the droplet vaporization time scales start at microseconds for nearly micron-sized droplets and increase to minutes for coarse droplets of 0.5 mm (500 μm). It is expected that these time scales will be much shorter, at high temperatures (in excess of 2000 °C) encountered in shock front. However, because of very high velocity, the residence time will be very short. Then, only droplets with vaporization time scales of microseconds or shorter will respond to shock energy extraction. The droplets of UFM (below 23 μm) will exhibit vaporization time scales of microseconds or lower at those temperatures.

The analysis indicates that UFM (below 23 μm) formed during the breakup process will be positioned to extract the energy from the shock by vaporization in terms of closely matching microsecond time scales. As seen, the time scales for coarse droplets are of the order of seconds; these droplets may contribute very little to the mitigation process if they are not fragmented. Based on the residence time scaling by the CFD modeling study, we find that even 100 μm droplets are not very well positioned for extracting energy by vaporization efficiently, since the residence time and vaporization time scales together will not match shock-induced vaporization. Unfortunately, these medium scale droplets of 100 μm will not be fragmented because the Weber number will be much lower than 12.

Based on energetics, as described by Salter [20] in the report, we need about 2.0 kg of water to balance the explosive energy of 1.0 kg of TNT. This is based on 2.25 MJ/kg of latent heat of water and 4.45 MJ/kg of explosive energy of TNT. As shown in the calculations presented here, the enormous number of droplets formed during the droplet breakup provides a huge surface area which accelerates the vaporization process. Besides vaporization, it is important to note the significant effect the drop concentration ($\sim 1 \times 10^{11}$ drops/kg) has on the speed of sound in a water–air mixture as reported by Karplus and Klinch [21] and Susan [22]. This will have a significant effect on the directions of propagation of shock waves.

4. Conclusions

Droplet breakup energies of coarse droplets of 0.5 mm were determined from the surface energies of both parent and child droplets. A breakup energy of ~18 J/kg was required to fragment a 0.5 mm parent droplet into 10,000 mono-dispersed ~23 μm droplets. This energy extraction due to fragmentation when compared to the vaporization energy of 2.25×10^6 J/kg is insignificant in weakening the shock. While the droplet deformation energy and curvature effects could increase the breakup energy, its overall contribution to the total energy extraction was not as significant as the vaporization enthalpy. However, there are far more important implications of the formation of blast-induced UFM droplets on the mitigation process. The analysis showed that there is a significant increase in the droplet vaporization rate with the 22-fold increase in surface area of the ~23 μm child droplets. Thus, the surface-to-volume ratio of the ultra fine droplets and their vaporization time scales of microseconds indicate they should be well positioned for shock energy extraction. The opportunity exists for further investigation, optimization, and integration of the blast-induced droplet break process for explosion mitigation technology.

Acknowledgement

This work was funded as part of the Office of Naval Research (ONR) Shipboard Fire Mitigation Thrust Program.

References

[1] G.G. Back, P.J. DiNenno, J.T. Leonard, R.L. Darwin, Full scale tests of water mist fire suppression systems for Navy Shipboard Machinery Spaces: phase I—unobstructed spaces, NRL/MR/6180-96-7830, US Naval Research Laboratory, ⟨http://stinet.dtic.mil⟩, March 8, 1996.
[2] G.G. Back, P.J. DiNenno, J.T. Leonard, R.L. Darwin, Full scale tests of water mist fire suppression systems for Navy Shipboard Machinery Spaces: phase II—obstructed spaces, NRL/MR/6180-96-7831, US Naval Research Laboratory, ⟨http://stinet.dtic.mil⟩, March 8, 1996.
[3] K. Kailasanath, P.A. Tatem, F.W. Williams, J. Mawhinney, Blast mitigation using water—a status report, NRL/MR/6400-02-8606, US Naval Research Laboratory, ⟨http://stinet.dtic.mil⟩, March 15, 2002.
[4] D. Schwer, K. Kailasanath, Blast mitigation by water mist (1)—simulation of confined blast waves, NRL/MR/6410-02-8636, US Naval Research Laboratory, ⟨http://stinet.dtic.mil⟩, August 16, 2002.
[5] D. Schwer, K. Kailasanath, Blast mitigation by water mist (2)—shock wave mitigation using glass particles and water droplets in shock tubes, NRL/MR/6410-03-8658, US Naval Research Laboratory, ⟨http://stinet.dtic.mil⟩, January 21, 2003.
[6] J.L. Bailey, M.S. Lindsay, D.A. Schwer, J.P. Farley, F.W. Williams, Blast mitigation using water mist, NRL/MR/6180-06-8933, US Naval Research Laboratory, ⟨http://stinet.dtic.mil⟩, January 18, 2006.
[7] H.D. Willauer, J.L. Bailey, F.W. Williams, Water mist suppression system analysis, NRL Letter Report 6180/0030, Chemistry Division, Code 6180, US Naval Research Laboratory, Washington, DC, 20375, February 7, 2006.
[8] A.H. Lefebvre, Atomization and Sprays, Hemisphere Publishing Corporation, Philadelphia, 1988.
[9] G.O. Thomas, On the conditions required for explosion mitigation by water sprays. Process safety and environmental protection, Trans. Inst. Chem. Eng. Part B 78 (2000) 339.
[10] S. Temkin, H.K. Mehta, Droplet drag in an accelerating and decelerating flow, J. Fluid Mech. 116 (1982) 297.
[11] J.R. Brenton, G.O. Thomas, Small-scale studies of water spray dynamics during explosion mitigation tests, I CHEM E Symposium Series No. 134, Hazards XII 39 (1994) 393.
[12] C.A. Chryssakis, D.N. Assaniss, A secondary atomization model for liquid droplet deformation and breakup under high Weber number conditions, in: ILASS Americas, 18th Annual Conference on Liquid Atomization and Spray Systems, Irvine, CA, May 2005.
[13] L.-P. Hslang, G.M. Faeth, Near-limit drop deformation and secondary breakup, Int. J. Multiphase Flow 18 (1992) 635.
[14] M. Pilch, C.A. Erdman, Use of breakup time data and velocity history data to predict the maximum size of stable fragments for acceleration-induced breakup of a liquid drop, Int. J. Multiphase Flow 13 (1987) 741.
[15] K.C. Adiga, R.F. Hatcher Jr., R.S. Sheinson, F.W. Williams, S. Ayers, A computational and experimental study of ultra fine water mist as a total flooding agent, Fire Saf. J. 42 (2007) 150.
[16] K.C. Adiga, Ultrafine water mist fire suppression technology, Fire Eng. (2005) 197.
[17] K.C. Adiga, R.F. Hatcher, E.W. Forssell, J.L. Scheffey, P.J. DiNenno, G.G. Back III, J.P. Farley, F.W. Williams, False deck testing of nanomist water mist systems,

in: Proceedings Halon Options Technical Working Conference, Albuquerque, NM, 2005.
[18] K.C. Adiga, R. Adiga, R.F. Hatcher, Fire suppression using water mist with ultra fine size droplets, US Patent 7,090,028, April 15, 2006.
[19] K.C. Adiga, R. Adiga, R.F. Hatcher, Method and device for production, extraction and delivery of mist with ultra fine droplets, US Patent 6,883,724, April 26, 2005.
[20] S.H. Salter, Why is water so good at suppressing the effects of explosions? UK Explosives Mitigation Workshop, RCMS, Shrivenham, 19 June 2002.
[21] H.B. Karplus, J.M. Clinch, Sound propagation in two-phase fluids, J. Acoust. Soc. Am. 36 (1964) 1040.
[22] W.K. Susan, Sound speed in liquid–gas mixtures' water–air and water–steam, J. Geol. Res. 82 (20) (1977).